

# Molecular dynamics of strongly coupled multichain Coulomb polymers in pure and salt-added Langevin fluids

Motohiko Tanaka

National Institute for Fusion Science, Oroshi-cho, Toki 509-5292, Japan

A. Yu Grosberg<sup>a)</sup> and Toyochi Tanaka

Massachusetts Institute of Technology, Cambridge, Massachusetts 02139

(Received 10 November 1998; accepted 27 January 1999)

The multichain effect and also the effect of added salt on randomly copolymerized charged polymers (polyampholytes) in a Langevin fluid are studied with the use of molecular dynamics simulations. The monomers of opposite signs tend to form loose complexes, which makes the Coulomb force attractive on average. With multichain polyampholytes, the typical state at high temperature is a container-bound one-phase state of separated chains with a substantial void among them. The association and dissociation processes occur repeatedly, with the former process a few times faster than the latter. A glass transition occurs when temperature is lowered. A compact and glassy globule in a segregated phase, which resembles that of a single-chain polyampholyte, is a typical state at low temperature due to the Coulomb force. The probability of losing this state is as low as  $P_{\text{dis}} \sim \exp(-N^{3/2})$ , with  $N$  the number of monomers. The critical temperature defined by overlapping of the chains increases with molecular weight and stiffness of the chains, and is less sensitive to the number of the chains. An alternate charge sequence makes a difference only when its block size is quite small. The addition of salt suppresses the formation of a dense globule by shielding the electric field; however, this is not effective when the salt ions are not allowed to penetrate well into the globule. © 1999 American Institute of Physics. [S0021-9606(99)51316-0]

## I. INTRODUCTION

Electrically charged polymers are interesting research objects in physics and chemistry. They combine the nature of a strongly coupled Coulomb system at room temperature due to microscopic scales on the Angstrom range with the peculiarities of the chainlike molecular structure. These polymers have a wide variety of industrial applications due to liquid-like plasticity and good solubility with respect to pure water and salt aqueous solutions.<sup>1</sup> In daily life, charged polymers are often encountered in the form of gels. In biological organisms they are also numerous, including proteins<sup>2</sup> and as nucleic acids of DNA and RNA.

Charged polymers are classified into two large groups, called *polyelectrolytes* and *polyampholytes*. The former type of polymer has a backbone that consists of monomers of one charge sign (apart from interleaving neutral monomers). This type, which is usually accompanied in solution by neutralizing counterions,<sup>3</sup> is widely utilized as industrial materials. DNA and RNA molecules in the living cells are also of that type. Polyampholytes, on the other hand, are the polymers that are composed of both positively and negatively charged monomers.<sup>4</sup> Importantly, polyampholytes are *heteropolymers*, and the combination of attraction and repulsion long-range Coulomb forces creates multiple frustrations.<sup>5</sup> Obviously, properties of polyampholytes depend on overall

*composition*, i.e., how many positively and negatively charged monomers are there in the chain. As with other heteropolymers, more delicate properties are determined by the specific *sequence* in which positive and negative monomers are connected one after another in the chain. Furthermore, this sequence may be *annealed* or *quenched* depending on the  $pK$  (ionization potential) of the monomers involved and on the pH in solution. An early study of polyampholytes was concerned mostly with the annealed ones, in analogy with proteins whose ionic characteristics depend on pH due to the presence of both acidic and basic components.<sup>4</sup> Recent studies have mostly been related to the quenched polyampholytes whose characteristics are independent of pH since their charge sequences are predetermined by synthesis chemistry. In a series of experimental works,<sup>4,6,7</sup> special emphasis was placed on the conformation and solubility of polyampholytes with respect to water and salt aqueous solutions.

Recent experimental activity in the field of polyampholytes was accompanied by the series of theoretical works. It was pointed out in the work<sup>8</sup> that the Debye-Hückel attraction effect between charge density fluctuations should exist and lead to compaction of typical quenched polyampholytes. This effect appears unusually sensitive to the overall charge of the chain, as it was shown first by Kantor and Kardar.<sup>9</sup> Specifically, a spherical globule is formed when the chain is neutral, but it becomes elongated or even adopts the necklace shape, when charge offset becomes of order or greater than  $\sqrt{N}$ ,  $N$  being the number of charged monomers. The most complete work in this direction<sup>10</sup> investigated

<sup>a)</sup>Permanent address: Institute of Biochemical Physics, Russian Academy of Sciences, Moscow 117977, Russia.

shape and stability of the polyampholyte globule in terms of a simple Flory theory. Recently, the multichain effect and the phase equilibrium in pure water and salt-added solution were examined,<sup>11</sup> and the single-chain theory was shown to apply only to an exponentially dilute solution of polyampholytes. Obviously, all the works deal with those properties of polyampholytes which are composition-dependent, but sequence insensitive. An attempt to look into sequence specific properties was undertaken in the work by Pande *et al.*<sup>12</sup>

Numerically, single-chain polyampholytes were first studied by a Monte Carlo simulation with the use of the lattice model,<sup>9</sup> and a few years later by a molecular dynamics (MD) simulation of the nonlattice type.<sup>13</sup> In the former, the effects of unbalanced charge and temperature were examined and found to be in reasonable agreement with the single-chain theory. The latter study, which examined the dynamical process and equilibrium properties, was the first to show the existence of a dense globular state at low temperature under the nonlattice model. It also demonstrated a hysteresis that the volume (i.e., the gyration radius) of the polyampholyte undergoes when the temperature changes slowly. This is the result of cooperation between the Coulomb and short-range attraction forces. The effect of an applied electric field on the stretching properties of polyampholytes was studied quite recently with a MD simulation<sup>14</sup> (note that this effect is sequence specific).

Owing to these experimental and theoretical studies, our understanding of polyampholytes has greatly advanced. From a numerical point of view, it is worthwhile extending the research from single-chain to multichain cases in order to know precisely how the results for the single-chain polyampholytes are related to the case of multichain polyampholytes,<sup>11</sup> which is the usual case for experiments with aqueous solutions. Specifically, we are interested in the dynamics of chain association and dissociation, stability of collapsed complexes, and occurrence of a glass transition. Other interesting points are to quantify the precise effect of charge sequence, molecular weight, and that of added salt on the properties of the polyampholytes. The present paper is devoted to numerical studies of these issues of isolated (container bound) polyampholytes by means of molecular dynamics simulations. Further study of multichain polyampholytes in the periodic system is described in a separate paper<sup>15</sup> with the use of the Ewald sum method.<sup>16,17</sup>

In this study, we adopt model polyampholytes that are comprised of various numbers of equal length chains, each of which contains between 16 and 64 charged monomers. These are the randomly copolymerized polyampholytes, whose charge sequences are randomized across the chains by shuffling the already charge-assigned monomers. We impose the condition that the sum of all the charges of the polyampholyte is null. (Counterions are not introduced, except for salt ions in Sec. IV.) In addition to the polyampholytes made of random copolymerization, we also performed a series of runs with alternate sequences in order to delineate the influence of the sequences. These results are described in Sec. III.

## II. THE EQUATIONS OF MOTION

In the molecular dynamics simulations of this paper, the position and velocity of the monomers evolve in time following the Newton-Langevin equations of motion,

$$m \frac{d\mathbf{v}_i}{dt} = \mathbf{F}_{LR}(\mathbf{r}_i) - \frac{3k_B T}{a^2} (2\mathbf{r}_i - \mathbf{r}_{i+1} - \mathbf{r}_{i-1}) + \mathbf{F}_{th} - \nu m \mathbf{v}_i, \quad (1)$$

$$\frac{d\mathbf{r}_i}{dt} = \mathbf{v}_i. \quad (2)$$

Here,  $\mathbf{r}_i$  and  $\mathbf{v}_i$  are the position and velocity of the  $i$ -th monomer ( $i = 1 \sim N$ ), respectively,  $m$  is the monomer mass,  $T$  the temperature,  $a$  the normalization length (which is close in value to the bond length of the monomer pairs), and  $\nu$  the friction constant. The Coulomb force  $\mathbf{F}_{LR}$ , which is an electrostatic long-range force, is obtained by summing over all the possible monomer pairs,

$$\mathbf{F}_{LR}(\mathbf{r}_i) = \sum_j \frac{Z_i Z_j e^2}{\epsilon |\mathbf{r}_i - \mathbf{r}_j|^2} \hat{\mathbf{r}}_{ij}, \quad (3)$$

where  $Z_i$  is a charge state ( $Z_i = \pm 1$ ),  $\epsilon$  the electrical permittivity, and  $\hat{\mathbf{r}}_{ij}$  a unit vector along the line ( $\mathbf{r}_i - \mathbf{r}_j$ ). In Eq. (1), a harmonic spring force of entropic nature is adopted to account for the connection of two adjacent monomers. The thermal force  $\mathbf{F}_{th}$  that exerts random kicks on the monomers is generated with the use of random numbers with a Gaussian distribution in each time step. The strength of the thermal kicks is controlled in such a way that the average kinetic energy of the monomer equals  $3/2 k_B T$ , in balance with the momentum absorption by the immobile solvent.<sup>13</sup> (Energy units are hereafter used in which the temperature  $T$  stands for  $k_B T$ , with  $k_B$  the Boltzmann constant.)

It should be noted that, with the use of normalized variables (with tildes),

$$\mathbf{r} = a \tilde{\mathbf{r}}, \quad \mathbf{v} = a \omega_p \tilde{\mathbf{v}}, \quad t = \omega_p^{-1} \tilde{t}, \quad (4)$$

the set of equations, Eqs. (1)–(3), are written explicitly by means of two nondimensional parameters,

$$\frac{d\tilde{\mathbf{v}}_i}{d\tilde{t}} = \mathbf{F}_{LR}(\tilde{\mathbf{r}}_i) - \frac{3}{4\pi\Gamma} (2\tilde{\mathbf{r}}_i - \tilde{\mathbf{r}}_{i+1} - \tilde{\mathbf{r}}_{i-1}) + \mathbf{F}_{th} - \xi \tilde{\mathbf{v}}_i, \quad (5)$$

$$\frac{d\tilde{\mathbf{r}}_i}{d\tilde{t}} = \tilde{\mathbf{v}}_i, \quad \mathbf{F}_{LR}(\tilde{\mathbf{r}}_i) = \frac{1}{4\pi} \sum_j \frac{Z_i Z_j}{|\tilde{\mathbf{r}}_i - \tilde{\mathbf{r}}_j|^2} \hat{\mathbf{r}}_{ij}. \quad (6)$$

These are the electrostatic coupling constant  $\Gamma = e^2/\epsilon a T$  and the friction constant  $\xi = \nu/\omega_p$ , where  $\omega_p = (4\pi n_0 e^2/\epsilon m)^{1/2}$  is the plasma frequency with  $n_0 \sim 1/2a^{-3}$  an average (positive) charge density. If we assume the  $\text{CH}_2$  monomer in pure water and at room temperature, i.e.,  $\epsilon \sim 80$  and  $a \sim 2 \text{ \AA}$ , the Coulomb energy prevails over thermal energy,  $\Gamma \sim 3.5$ , and  $\omega_p \sim 9.8 \times 10^{12} \text{ s}^{-1}$  ( $\omega_p^{-1} \sim 0.1 \text{ ps}$ ). Each monomer has a rigid sphere that the other monomer cannot penetrate into; it is elastically reflected upon entering the distance called the exclusion radius  $a_{col}$ . The stiffness of the chains in our simulation yields  $v/a^3 = (\pi/6)(a_{col}/a)^3 \sim 0.004 - 0.065$  for  $a_{col} = 0.2a - 0.5a$ , where  $v = (4\pi/3)(a_{col}/2)^3$  is the exclusion

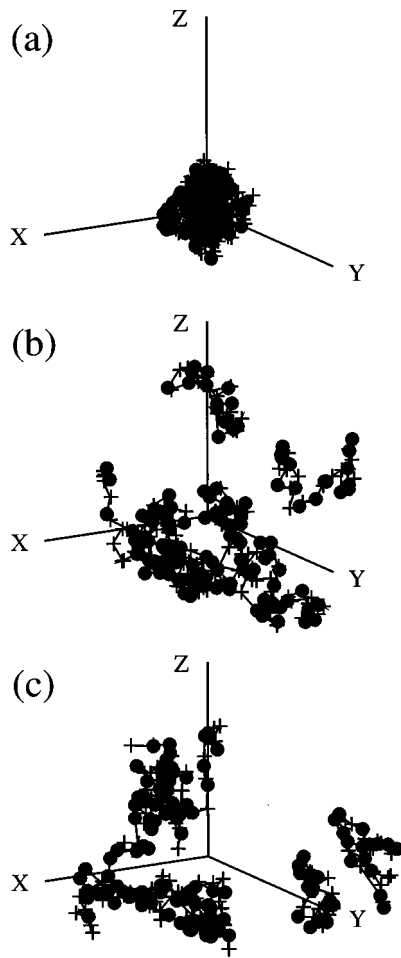


FIG. 1. Time evolution of a randomly copolymerized multichain polyampholyte composed of eight 32-mer chains, for temperature  $T/T_0=1/2$ , at times (a)  $\omega_p t=0$ , (b)  $\omega_p t=300$ , and (c)  $\omega_p t=600$ . The monomers are confined in a spherical domain of radius  $R=21a$ . The + and ● show the monomers of positive and negative charges, respectively, and the exclusion radius of the monomer is  $a_{\text{col}}=0.5a$ .

volume of the monomer. The chosen stiffness well represents those values obtained by laboratory experiments, i.e.,  $v/a^3 \leq 0.2$  for most flexible monomers, and  $v/a^3 \sim 0.003$  for double helix DNA.<sup>18</sup>

Other parameters that control the properties of polyampholytes are the charge sequences, the molecular weight, and the number of chains that comprise the polyampholytes. These parameters are systematically changed in the simulation runs in Secs. III and IV. The step of time integration is  $\Delta t=0.01\omega_p^{-1}$ , which is adequate to resolve the fastest motions. The standard parameters  $a_{\text{col}}=0.5a$  and  $\nu=0.03\omega_p$  are used unless otherwise specified.

In the following sections, we deal with the multichain polyampholytes that are confined within a spherical shell of radius  $R=21a$ , which is filled with a Langevin fluid. (Refer to Ref. 15 for multichain polyampholytes in the periodic system.) The monomers hitting the boundary surface are reflected elastically, but the electric field is not distorted there. Except for the alternate sequences in Sec. III, the polyampholytes used in the following sections consist of randomly copolymerized quenched chains of six 32-mers, with the constraint of overall charge neutrality. Thus, an individual

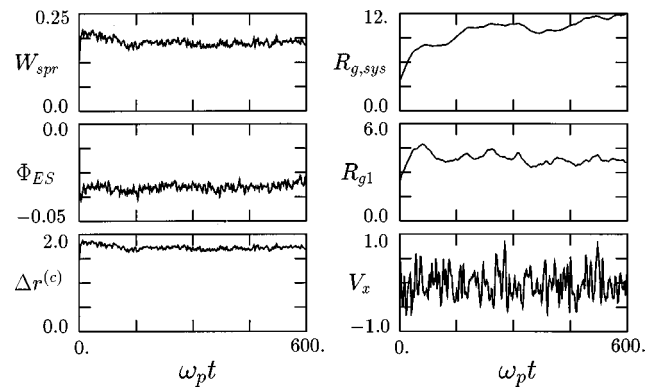


FIG. 2. Time history of various quantities for the polyampholyte depicted in Fig. 1: the average elastic energy per monomer  $W_{\text{spr}}$ , the Coulomb energy per monomer normalized by the base thermal energy  $\Phi_{ES}/T_0$ , the average bond length of connected monomers  $\Delta r^{(c)}$ , the system gyration radius including all the monomers  $R_{g,\text{sys}}$ , the average gyration radius of the chains  $R_{g1}$ , and the  $x$ -component velocity  $V_x$  of an individual monomer.

chain is not neutral, having typically a charge of order  $\pm e\sqrt{N_1}$ , where  $N_1$  is the number of monomers on a chain.

### III. MULTICHAIN POLYAMPHOLYTES IN PURE SOLVENTS

#### A. Time evolution of multichain polyampholytes

A typical time evolution of a multichain polyampholyte is shown by the bird's-eye view snapshots of Fig. 1. Here, the polyampholyte is composed of eight flexible chains of 32-mers with an exclusion radius of  $a_{\text{col}}=0.5a$ . The temperature is  $T/T_0=1/2$ , where  $T_0$  is the base temperature for which the coupling constant becomes unity, i.e.,  $\Gamma_0=e^2/\epsilon a T_0=1$ . The initial configuration of a small droplet expands to the separated chains in Fig. 1(b) after a time  $\tau_{\text{eq}} \sim 300\omega_p^{-1}$ . There is a large void among the chains. The relative positions of the chains continue to fluctuate due to random thermal kicks in the Langevin fluid. Some of the chains remain entangled for a period of time and then are separated for another period of time, as seen in Figs. 1(b) and 1(c). The above relaxation time corresponds to  $\tau_{\text{eq}} \sim 30$  ps for the CH<sub>2</sub> monomer in pure water ( $\epsilon=80$ ).

Figure 2 shows the time history of several quantities for the run depicted in Fig. 1. The average spring energy per monomer,  $W_{\text{spr}}=(3T/2a^2)\langle(\Delta r^{(c)})^2\rangle$ , in the top-left panel adjusts itself and levels off to the equilibrium value  $3/2T$ , which equals the average kinetic energy. This manifests equipartition of the oscillation energy. The middle-left panel shows the Coulomb energy per monomer,  $\Phi_{ES}$ , normalized by the base thermal energy  $T_0$ , defined as

$$\Phi_{ES}=\frac{1}{N}\sum_i\sum_{j>i}\frac{Z_i Z_j e^2}{\epsilon|\mathbf{r}_i-\mathbf{r}_j|}. \quad (7)$$

A large change in the Coulomb energy takes place in the initial transient stage because local charge rearrangement occurs for which the deviation  $\Delta\Phi_{ES} \sim e^2/\epsilon r_{ij}$  is relatively large. Subsequent changes are due to the global relaxation of the conformations, which are inversely proportional to the size of the polyampholyte and small in magnitude. The bond

length between the connected monomers  $\Delta r^{(c)}$  remains almost constant although they are loosely connected by harmonic springs.

The top-right panel depicts the *system* gyration radius  $R_{g,\text{sys}}$  that includes all the monomers of the polyampholyte, and the middle-right panel shows the average of the gyration radii of the chains  $R_{g1}$ . These radii are defined, respectively, as

$$R_{g,\text{sys}} = \left( \frac{1}{N} \sum_{j=1}^N (\mathbf{r}_j - \langle \mathbf{r} \rangle)^2 \right)^{1/2}, \quad (8)$$

$$R_{g1} = \frac{1}{N_c} \sum_{s=1}^{N_c} \left( \frac{1}{N_1} \sum_{j=1}^{N_1} (\mathbf{r}_j - \langle \mathbf{r}_s \rangle)^2 \right)^{1/2}, \quad (9)$$

where  $N$  is the number of all the monomers, and  $N_c$  is the number of chains, i.e.,  $N = 192$ ,  $N_c = 6$ , and  $N_1 = 32$ . As earlier noted, individual chains have a small net charge under random copolymerization. The system gyration radius increases to  $R_{g,\text{sys}} \sim 12a$  on the time scale  $\tau_{\text{eq}} \sim 300\omega_p^{-1}$ , which is the value allowed for a system whose radius is limited to  $R = 21a$ . The diffusion speed of the chains can be deduced by  $V_{\text{diff}} = dR_{g,\text{sys}}/dt$ . It becomes  $\sim 0.12a\omega_p$  in the early time  $t < 50\omega_p^{-1}$ , which is about one third that of the thermal speed  $v_{th} = (3/4\pi\Gamma)^{1/2}$  ( $\Gamma = T_0/T$ ). Except for this early stage, the diffusion speed is  $V_{\text{diff}} \sim 0.02a\omega_p$  on average, which is about 5% that of the thermal speed.

As stated above, the slow changes in the Coulomb energy and the system gyration radius occur simultaneously. On the other hand, the average gyration radius of the chains oscillates around the value  $R_{g1} \sim 4a$ . The velocity  $V_x$  of an individual monomer exhibits amplitude oscillations whose period is longer than the friction time  $\nu^{-1}$ . This should correspond to large structure fluctuations of the polyampholyte, since fast oscillations without energy sustainment are damped and wiped out in a Langevin fluid.

The temperature variation of the typical relaxed conformations of the multichain polyampholyte is shown in Fig. 3 for three temperatures: (a)  $T/T_0 = 1$ , (b)  $T/T_0 = 1/4$ , and (c)  $T/T_0 = 1/8$ . All the plots are drawn on the same scale, with the size of the negative monomers (dots) prorated. At high temperature, i.e., case (a), the polyampholyte is made up of elongated coils whose mass centers distribute homogeneously in the finite domain. As the temperature is lowered to that of case (b), there occurs a change from a one-phase state with scattered coils to a segregated phase with globules; their life in pairs is still short and mostly they live separately. When the temperature is further lowered as in case (c), the chains form a compact globule that cannot be distinguished from the one consisting of a single continuous chain. Note that the globule keeps a spherical shape having a nearly fixed radius and a distinct surface, with not a single monomer straying outside. As will be mentioned later, the monomers in a compact globule of Fig. 3(c) continue to vibrate under thermal agitations from surrounding medium. These evidences indicate that the compact globule is in the *glass* state, which is virtually a natural state of the low temperature polyampholyte,<sup>8</sup> irrespective of the boundary conditions of the domain.

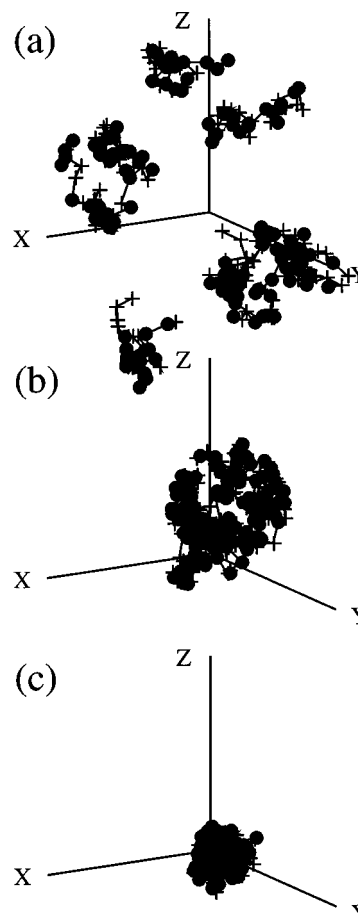


FIG. 3. Typical relaxed conformations of eight 32-mer polyampholyte at  $\omega_p t = 600$ , for temperatures (a)  $T/T_0 = 1$ , (b)  $T/T_0 = 1/4$ , and (c)  $T/T_0 = 1/8$ . A gradual morphological change occurs from the one-phase state with separated chains of (a) to the segregated phase with a collapsed and dense globule of (c) around  $T/T_0 \sim 0.3$ . The monomers are confined in a spherical domain of radius  $R = 21a$ , and the exclusion radius of the monomer is  $a_{\text{col}} = 0.5a$ .

We note here that freezing is much easier to achieve on the lattice than in any off-lattice systems. The final state of the folding process with the use of the lattice model (of a small size) appears to be well defined due to such quantization that the energy gap between adjacent levels near the energy minimum is set a little too large to allow for thermal fluctuations. In this regard, off-lattice models like molecular dynamic simulations have obvious advantages compared to lattice models to study a thermally fluctuating state adopted by the chains. On the other hand, the very concept of freezing needs careful formulation and definition for any off-lattice systems.

## B. Statistical properties of multichain polyampholytes

Figure 4 highlights the effect of the Coulomb force by displaying side by side the results for charged and non-charged polymers. Each data point in the figure (and also in the following figures with the same format, viz., Figs. 5–8, 11 and 12) is an average over 20 independent runs with polyampholytes of different charge sequences (random but overall charge neutrality) and initial conformations. In panels (a) and (b) of Fig. 4, the system and average gyration radii

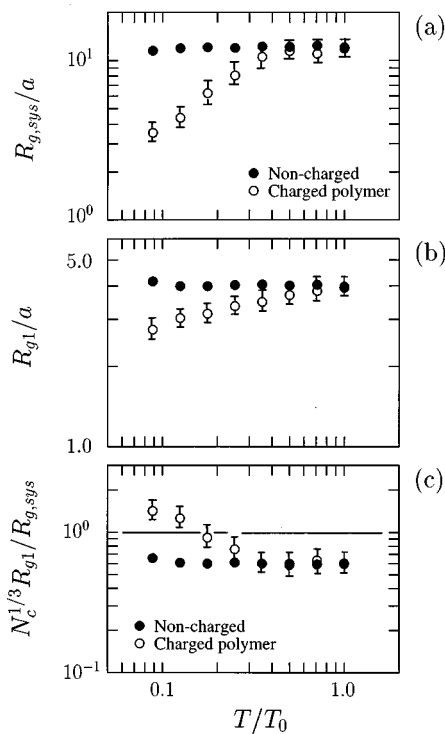


FIG. 4. Effect of the Coulomb force on structure formation of polyampholytes, as seen in differences between the noncharged polymers and charged polymers of random copolymerization. The polymers are composed of six 32-mers, and the panels show (a) the system gyration radius  $R_{g,sys}$  including all the monomers, (b) the average gyration radius of the chains  $R_{g1}$ , and (c) the filling index  $N_c^{1/3}R_{g1}/R_{g,sys}$  which indicates chain overlapping, where  $N_c$  is the number of chains.

are shown, respectively, as functions of temperature. Here, the polymers are comprised of six 32-mers. For the non-charged polymers, neither of the two gyration radii  $R_{g,sys}$  or  $R_{g1}$  depends on temperature. Insensitivity of the gyration radii of individual chains on temperature is expected for the entropic elasticity adopted in Eq. (1). The charged polymers here are quenched polyampholytes of random copolymerization, for which deviations from the noncharged polymers are evident in the low temperature regime  $T/T_0 < 1$  where the Coulomb energy much exceeds the thermal energy. An error bar shows the extent in which 60% of the data points exist. On the other hand, differences are small at high temperature. The figure clearly shows that the Coulomb force is attractive on average for randomly copolymerized polyampholytes. (Qualitatively similar results are found also in the periodic system.<sup>15</sup>)

Figure 4(c) depicts the *filling index* that indicates the degree of chain overlapping or entanglement, defined as

$$\zeta \equiv N_c^{1/3} R_{g1} / R_{g,sys} \quad (10)$$

The criterion that the polyampholyte resides in a segregated phase and is non-soluble with respect to the solvent is given by the condition  $\zeta \geq 1$ . This corresponds to close overlapping of the chains and the network formation. In the opposite condition,  $\zeta < 1$ , the polyampholyte is considered to be transparent for the light scattering experiments and soluble to the solvent. The filling index for the polyampholyte in Fig. 4(c) is larger than unity at low temperature. The critical tempera-

TABLE I. Top: The fraction of spatially nearest monomer pairs having equal-sign charges (denoted by  $+/+-$ ) and opposite sign charges ( $+/-+$ ), and the average distance  $\Delta r$  between such pairs, for randomly copolymerized multichain polyampholytes (six 32-mers) of overall charge neutrality. Bottom: The fraction of equal/opposite-sign monomers that are located within a sphere of radius  $\Delta r < 1.5a$ .

$T/T_0$	( $+/+-$ )	( $+/-+$ )	$\Delta r^{(++)}$	$\Delta r^{(+-)}$	$N(\Delta r < 1.5a)$
1.00	47%	53%	1.67	1.61	
0.50	44%	56%	1.71	1.49	
0.25	36%	64%	1.46	1.24	
0.125	31%	69%	1.24	0.97	
1.00	44%	56%	...	...	1.15
0.50	41%	59%	...	...	1.19
0.25	40%	60%	...	...	1.83
0.125	43%	57%	...	...	3.40

ture defined by the condition  $\zeta = 1$  is  $T_*/T_0 \sim 0.17$  for the standard parameters. This coincides with the observed temperature in the molecular dynamics simulations at which the one-phase state (separated chains) replaces the segregated phase (globule). On the other hand, the noncharged polymers are soluble,  $\zeta < 1$ , for the entire temperature range shown in the figure. These features are consistent with the theory of multichain polyampholytes.<sup>11</sup>

The attractive nature of the Coulomb force for polyampholytes is also found in Table I. At low temperature  $T/T_0 \leq 1/4$ , the possibility of opposite-sign charges being the nearest monomer pairs (not necessarily the connected monomer pairs) is significantly larger than that of equal-sign charges. Also, the distance between monomers of opposite-sign charges is smaller than that with equal-sign charges, which implies the formation of loose complexes of positive and negative monomers. At high temperature  $T/T_0 = 1$ , the difference between the charge pairs is small, which is consistent with the similarity of charged and noncharged polymers at a similar temperature shown in Fig. 4. When we look at a sphere of radius  $1.5a$  centered on a monomer, the average number of surrounding monomers having different sign charges is always larger than that with equal-sign charges, as shown in the bottom part of Table I.

Figure 5 shows the effect of chain stiffness on the size of polyampholytes. The size of a flexible polyampholyte is always larger than that of a stiff one at a given temperature, except at high temperature where the system gyration radius approaches the limit set by the domain size. The system gyration radius is an increasing function of temperature:  $R_{g,sys} \propto T^{0.7}$  for flexible chains, and  $R_{g,sys} \propto T^{1.1}$  for stiff chains. These dependences for multichain polyampholytes are more sensitive than the scaling  $R_g \propto T^{1/3}$  for single-chain polyampholytes.<sup>13</sup> This is attributed to the growth of a large void space among the chains.

As the multichain effect of polyampholytes preferentially affects their global size, the filling index for the stiff chains becomes larger than that for the flexible chains. The critical temperature for chain overlapping to occur shifts from  $T_*/T_0 \sim 0.17$  for the flexible chains to  $T_*/T_0 \sim 0.33$  for the stiff chains.

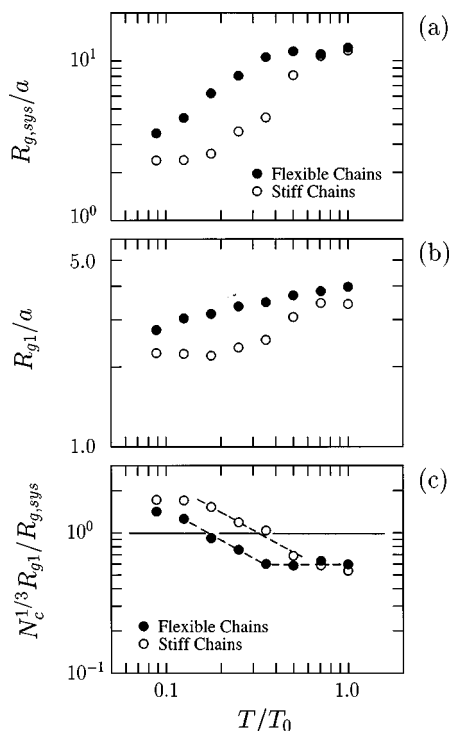


FIG. 5. Effect of chain stiffness, for six 32-mer polyampholytes of random copolymerization. The flexible chains consist of monomers with exclusion radius  $a_{col}=0.5a$ , and the stiff ones have  $a_{col}=0.2a$ . The panels show (a) the system gyration radius  $R_{g,sys}$ , (b) the average gyration radius of the chains  $R_{g1}$ , and (c) the filling index  $N_c^{1/3}R_{g1}/R_{g,sys}$ .

The Coulomb energy per monomer defined by Eq. (7) is depicted in Fig. 6(a) as a function of temperature. By comparison of Figs. 5 and 6, the Coulomb energy is found to be inversely proportional to an average of the gyration radii of individual chains,  $\Phi_{ES} \propto R_{g1}^{-1}$ . This is quite understandable since the major contribution to the Coulomb energy arises from the adjacent monomer pairs whose distance is nearly

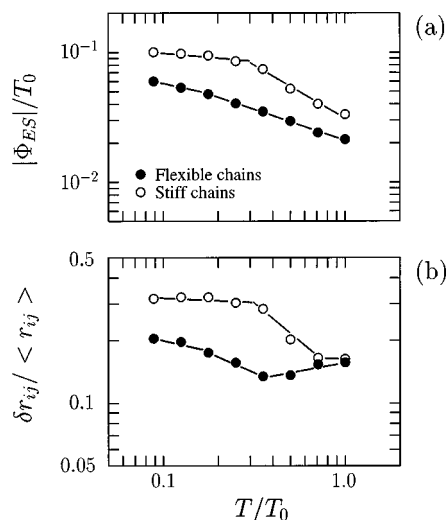


FIG. 6. (a) Coulomb energy per monomer normalized by the base thermal energy  $\Phi_{ES}/T_0$  defined by Eq. (7); (b) deviation of the monomer distances  $\delta r_{ij}$  normalized by the average monomer distance  $\langle r_{ij} \rangle$ , for the flexible and stiff chains in Fig. 5.

proportional to the gyration radius  $R_{g1}$  in the one-phase state. The contribution of the global conformation to  $\Phi_{ES}$  is small, but is nevertheless decisive for the large-scale structure formation.

Very interestingly, the slope of the curve of the Coulomb energy in Fig. 6(a) changes suddenly around  $T/T_0 \sim 0.18$  for the polyampholytes of flexible chains, and around  $T/T_0 \sim 0.30$  for those of stiff chains. This leads to a jump in the heat capacity  $C_{coul} = \partial \Phi_{ES} / \partial T$  at those temperatures, indicating occurrence of a phase transition for multichain polyampholytes. This transition, which is considered to be a *glass transition*, occurs at the temperature  $T_*$  where the morphological change between the one-phase state and the segregated phase takes place.

The phase transition is also identified in Fig. 6(b) which shows the time deviation of the monomer distance,

$$\Delta_{ij} = \frac{2}{N(N-1)} \sum_i \sum_{j>i} \delta r_{ij} / \langle r_{ij} \rangle. \quad (11)$$

Here,  $\delta r_{ij}$  is the time deviation of the monomer distance  $r_{ij}$  between the  $i$ -th and  $j$ -th monomers. The summation is made over all possible pairs between  $N$  monomers. The ratio decreases gradually as the temperature increases or is rather constant at low temperature,  $T/T_0 \leq 0.18$  for the flexible chains, and  $T/T_0 \leq 0.30$  for the stiff chains. We note that these coincide with the transition temperature  $T_*$ , which is defined by  $\zeta=1$  in Fig. 5(c), and that of the electrostatic energy in Fig. 6(a). The chains form a globule below  $T_*$  as inferred from Fig. 5(c), but the deviation  $\delta r_{ij}$  is appreciable (20%–30%) in comparison with the average distance  $\langle r_{ij} \rangle$ . This feature is characteristic of the glass phase. At the middle temperature, the ratio  $\Delta_{ij}$  begins to decrease more rapidly due to dissociation of the chains, i.e., inflation of polyampholytes. Then, the ratio turns into an increase for  $T/T_0 \geq 0.35$ , since the deviation of the distance  $\delta r_{ij}$  grows due to thermal motion. For stiff chains, similar changes are seen where everything shifts to the higher temperature side.

### C. The effect of alternate sequences

It is predicted that a polyampholyte comprised of chains of alternate sequences has less of a tendency to make neutral complexes, and thus is more easily soluble in water.<sup>11</sup> To examine such effects with alternate sequences, a series of molecular dynamics simulations are performed, in which each of the six 32-mer chains is composed of alternating blocks of positively and negatively charged monomers. The length of the block (the number of monomers in a block) is taken to be one, two, and then four.

Figure 7 shows that polyampholytes of complete alternating sequence with a block length of unity (+−+−...) have a larger system gyration radius than those with a block length two and four in the Coulomb phase, for which  $T/T_0 < 0.4$  for the flexible polyampholytes [cf. Fig. 4(a)]. For chains with large block lengths, we find complexes of positive and negative blocks. The gyration radius for the alternate sequence with a block length four is already close to that for the randomly copolymerized sequence described in Sec. III B.

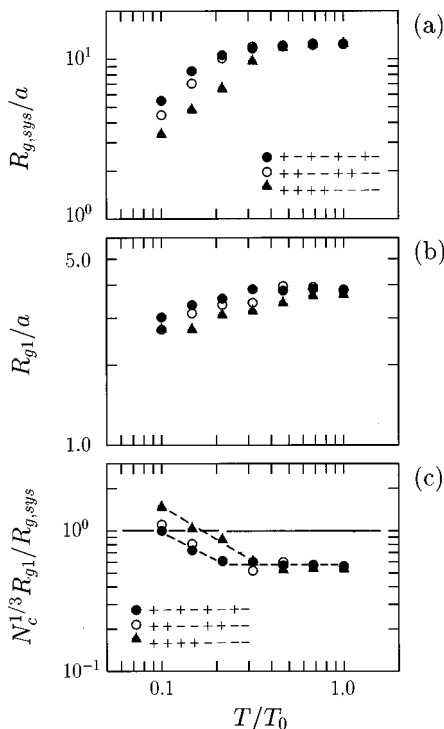


FIG. 7. Dependence on charge sequences, depicted by three series of runs, in which each of the six 32-mer chains has block size of equal-sign charges of one, two, and then four. The panels show (a) the system gyration radius  $R_{g,sys}$ , (b) the average gyration radius of the chains  $R_{g1}$ , and (c) the filling index  $N_c^{1/3} R_{g1}/R_{g,sys}$ .

The average of the gyration radii of individual chains  $R_{g1}$  in Fig. 7(b) depends on the sequence, which is reduced as the block size of one charge-sign becomes large in the Coulomb phase. The filling index  $\zeta = N_c^{1/3} R_{g1}/R_{g,sys}$  in Fig. 7(c) becomes large as the block length increases from one to four. Quite remarkably, in terms of the filling index, a polyampholyte with alternate sequence of block length four behaves just like one synthesized by random copolymerization. Thus, the charge sequence affects polyampholyte properties significantly only if it is completely alternate.

#### D. The effect of finite/infinite domains

The diffusion of polyampholyte chains at high temperature is blocked if the computational domain is surrounded by a boundary wall. This is a usual situation for polyampholytes in a solution. On the other hand, it is physically an interesting question whether the globular state at low temperature requires a closed domain of finite volume.

Figure 8 compares runs with finite and infinite domains. The polyampholytes here are again composed of six 32-mers of random copolymerization (overall charge neutrality), and each data point is obtained by averaging 20 independent runs with different random sequences and initial conformations. For polyampholytes in an infinite volume (filled circles), the upper two data points in Fig. 8(a) keep on growing with time (shown with arrows). However, the lower two points residing at  $T/T_0 \leq 1/8$  remain there stationary in time. Moreover, the latter points superimpose quite well on the data points for the finite volume.

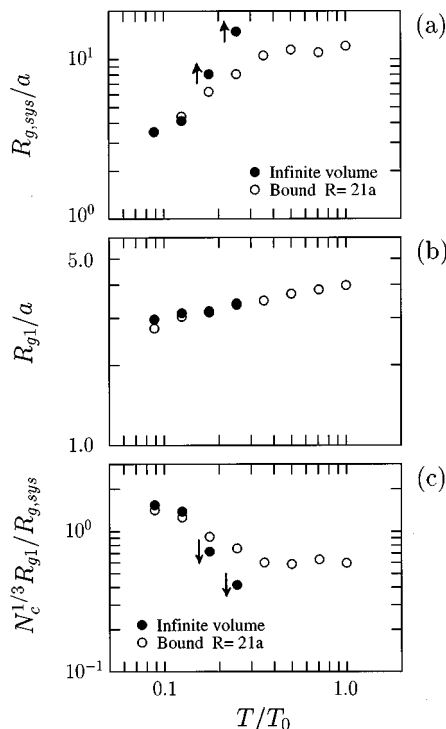


FIG. 8. (a) Effect of the domain size (boundary condition) on randomly copolymerized multichain polyampholytes (six 32-mers), for the case with infinite volume and the case with finite volume of a sphere of radius  $R = 21a$ . The panels show (a) the system gyration radius  $R_{g,sys}$ , (b) the average gyration radius of the chains  $R_{g1}$ , and (c) the filling index  $N_c^{1/3} R_{g1}/R_{g,sys}$ . The lower two dots at  $T/T_0 < 0.2$  for the infinite volume case of panel (a) are stationary, while the higher two dots increase steadily in time.

These results are not strange, since the globule obtained in the low temperature regime has a distinct surface without any monomers straying outside of the globule, irrespectively of the boundary conditions of the domain. This point is further confirmed by special long runs that continue up to 30 relaxation times,  $15000\omega_p^{-1}$ , of the six 32-mer polyampholyte chains. The time history of the system gyration radius is shown in Fig. 9 for the temperatures (a)  $T/T_0 = 1/2$ , (b)  $T/T_0 = 1/4$ , and (c)  $T/T_0 = 1/8$ . The domain is limited by a spherical wall of radius  $R = 21a$  except for the run in Fig. 9(d), for which the domain is infinite. Initial conformations of highly stretched threads of randomly copolymerized chains with overall charge neutrality are purposely chosen, to avoid artificial trapping of the conformations in a small volume.

The conformations for the medium temperatures,  $T/T_0 = 1/2$  and  $1/4$ , shown in Figs. 9(a) and 9(b), are the wall-stabilized ones in which the monomers are reflected inward by the elastic wall. Without the wall, infinite diffusion of monomers takes place, and a bound state is not obtained for these temperatures. We see repetition of the dissociation and association processes of the chains, starting at  $t \sim 2500\omega_p^{-1}$  and  $10000\omega_p^{-1}$  in Fig. 9(b). The inflation speed is deduced to be  $dR_{g,sys}/dt \sim 1.2 \times 10^{-3} a\omega_p$ , whereas the collapse speed is  $-2.6 \times 10^{-3} a\omega_p$ . Thus, the association process is about twice as fast as the dissociation process for the medium temperature  $T/T_0 \geq 1/4$ .

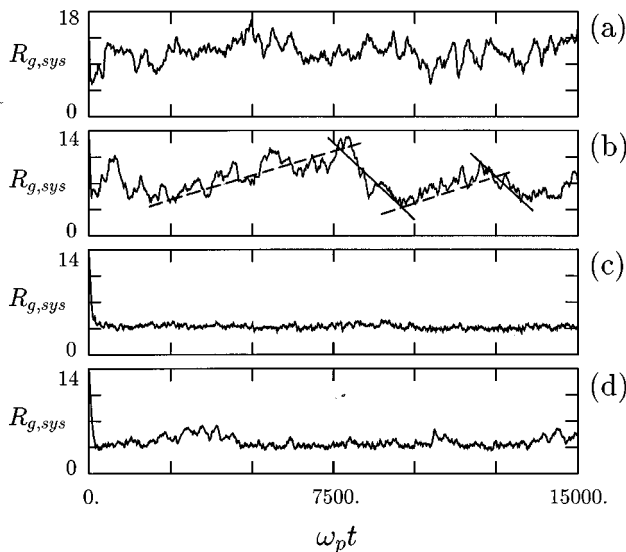


FIG. 9. Long-time history of the system gyration radius  $R_{g,sys}$  for the randomly copolymerized polyampholytes of Fig. 8 with temperatures (a)  $T/T_0=1/2$ , (b)  $T/T_0=1/4$ , and (c) and (d)  $T/T_0=1/8$ . The simulation domain through (a) and (c) is limited by a sphere of radius  $R=21a$ , whereas the domain for (d) is infinite.

We also notice, by comparing Figs. 9(c) and 9(d), that both of the system gyration radii for the closed and open systems at low temperature  $T/T_0=1/8$  are kept small, and are not much affected by the presence of the boundary wall. There, the polyampholyte forms a dense globule which remains stationary for times  $t > 500\omega_p^{-1}$ . The compact globule, which has the characteristics of glass, is thus regarded as a natural state of a low temperature polyampholyte.

The attractive nature of the Coulomb interactions is again verified by the special run in Fig. 10, where the monomer charges of a randomly copolymerized polyampholyte (six 32-mers) are suddenly reset to zero at time  $t = 4500\omega_p^{-1}$ . The time history of the system gyration radius in the top frame shows that the globule that has remained stationary is quickly destroyed, since the chains are no longer under the influence of the Coulomb force. Otherwise, the globule remains compact, as shown in Fig. 9(c). The scatter plots of Fig. 10 labeled (a) and (b) depict, respectively, the conformation with the Coulomb force inclusive and that after the Coulomb force has been switched off. It is interesting that the Coulomb force is strong enough to put the polyampholyte chains together at low temperature, without aid of the boundary wall. However, chain entanglement without actual bonds is unable to prevent the globule from being destroyed.

The stationary globular state at low temperature is thought to arise from enhanced stability by charge pairing, as shown in Table I. An increase in temperature removes the pairing, and the globular state is lost by thermal agitation. The above process may be theoretically treated in the following manner. If we treat the chains to lowest order as an assembly of charged particles without internal structures, then the essential part of the free energy may be approximated by adding the Coulomb energy to the free energy of the ideal gas,<sup>19</sup>

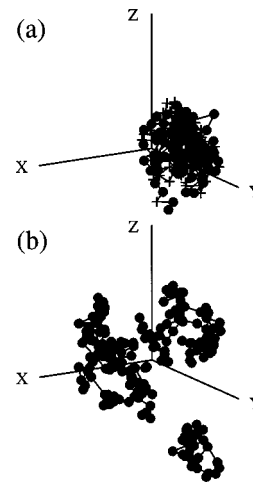
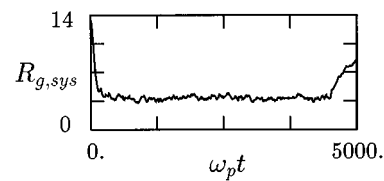


FIG. 10. Time history of the system gyration radius  $R_{g,sys}$  of a special run in which the monomer charges of the randomly copolymerized polyampholyte with temperature  $T/T_0=1/8$  of Fig. 9(b) are suddenly reset to zero at time  $t=4500\omega_p^{-1}$ . The scatter plots show their conformations at (a)  $t = 4000\omega_p^{-1}$  and (b)  $t = 5000\omega_p^{-1}$ .

$$F = NT \log\left(\frac{N/V}{n_Q} - 1\right) + U_{coul}, \quad (12)$$

$$U_{coul} = -A/\epsilon R \sim -A/\epsilon V^{1/3}.$$

Here, the coefficient is positive,  $A \sim (e^2 N_1) N_c = e^2 N > 0$ , due to the attractive nature of the Coulomb force among the chains. [Inclusion of the chain free energy is desirable in Eq. (12), but a free energy maximum occurring at finite volume may not be much affected since  $F$  becomes negative infinite both at  $V=0$  and  $V=\infty$ .] Notably, the free energy given by Eq. (12) possesses a maximum at an intermediate radius  $R$ . If we differentiate the free energy in terms of the radius  $R$  and equate it to zero, we get

$$R_0(T) = [V_0(T)]^{1/3} = A/\epsilon NT \sim a\Gamma \quad (\Gamma = T_0/T). \quad (13)$$

This reveals that the initial conformation starting with a small radius compared to  $R_0(T)$ , or the chains initially located within that distance, collapse to a single compact globule at low temperature. Moreover, the radius of bifurcation  $R = R_0(T) \sim a(T_0/T)$  increases when the temperature is lowered, which makes it possible for more initial conformations and chains to collapse to the globule. [It is found by molecular dynamics simulations that, by cooling homogeneous solution of polyampholyte, multiglobule phase is first obtained. In this case, the initial conformation includes the chains that are separated from the others for more than the distance

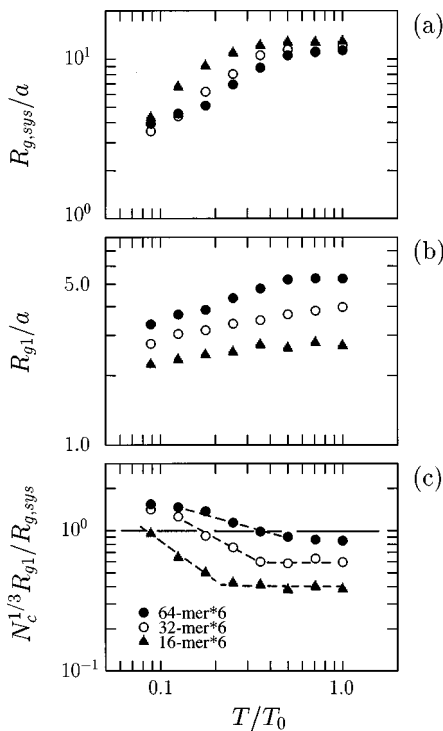


FIG. 11. Dependence on the length (molecular weight) of the chains, for randomly copolymerized polyampholytes. The number of chains is kept at six, and the panels show (a) the system gyration radius  $R_{g,sys}$ , (b) the average gyration radius of the chains  $R_{g1}$ , and (c) the filling index  $N_c^{1/3} R_{g1}/R_{g,sys}$ .

$R_0(T)$ .] All of these points, including the value of  $R_0$ , are in good agreement with the molecular dynamics simulation results.

Finally, we show that the probability for the polyampholyte chains to escape from the compact globule is virtually eliminated at low temperature. For low temperatures  $T/T_0 \leq 0.1$ , the intermonomer distance, especially that of the positive and negative pairs, becomes very small, as shown in Table I. The Coulomb energy is dominated by the attractive part. Then, the leading term of the energy gap between the globular state and the one-phase state of scattered coils is given by

$$\Delta E = e^2 N / \epsilon \lambda_D \sim e^3 N^{3/2} / \epsilon^{3/2} T^{1/2} R^{3/2}, \quad (14)$$

where the Debye length is  $\lambda_D = (\epsilon T / 4\pi n_0 e^2)^{1/2}$  and  $R^3 n_0 \cong N$ . Then, the probability for the globule to be destroyed by random thermal agitation is given by

$$P_{dis} = \exp(-\Delta E/T) \sim \exp(-e^3 N^{3/2} / \epsilon^{3/2} T^{3/2} R^{3/2}) \\ \cong \exp[-(a\Gamma/R)^{3/2} N^{3/2}]. \quad (15)$$

Here, the electrostatic coupling constant  $\Gamma = (T/T_0)^{-1}$  varies inversely with the temperature  $T$ . An important thing in Eq. (15) is its scaling with respect to the number of monomers  $N$ . For the typical parameters of a low temperature globule,  $\Gamma = 8$  and  $R/a \sim 3$ , the argument of the exponential function

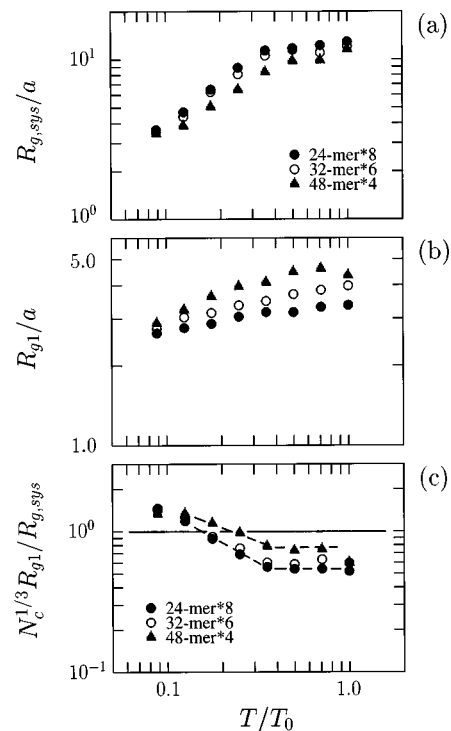


FIG. 12. Dependence on the number of chains, for randomly copolymerized polyampholytes. The total number of monomers is kept at 192, and the panels show (a) the system gyration radius  $R_{g,sys}$ , (b) the average gyration radius of the chains  $R_{g1}$ , and (c) the filling index  $N_c^{1/3} R_{g1}/R_{g,sys}$ .

becomes  $4.4N^{3/2}$ . Thus, any reasonable number of monomers for the chains to be regarded as a polymer yields a probability that is extremely small,

$$P_{dis} \propto \exp(-N^{3/2}) \ll 1. \quad (16)$$

This means that once a compact globule is formed at low temperature, it will fall apart only after an astronomically long period of time.

### E. Dependence on molecular weight

Figure 11 shows the effect of the length (molecular weight  $M_w$ ) of the chains on the radius of multichain polyampholytes made by random copolymerization with overall charge neutrality. In the medium temperature regime, the system gyration radius becomes larger for smaller molecular weight, scaling roughly as  $R_{g,sys} \sim M_w^{-1/2}$ . The average of the gyration radii of individual chains  $R_{g1}$  behaves like that of a single-chain polyampholyte.<sup>13</sup> At high temperature, it scales as  $R_{g1} \sim M_w^{1/2}$ , although the radius is only a fraction of that of the Gaussian coil. The filling index in Fig. 11(c) shifts upward with increase in the molecular weight of the chains. The critical temperature that separates the one-phase state and the segregated phase is  $T_*/T_0 \sim 0.082$ , 0.17, and 0.35 for the chains with 16-, 32-, and 64-mers, respectively. This is well fitted by the power law,  $T_*/T_0 \sim M_w^{1.04}$ . Therefore, the polyampholyte consisting of longer chains becomes more difficult to dissolve in neutral solvents.

On the other hand, the dependence on the number of chains is present but less in extent in Fig. 12, where the number (192) of monomers is fixed, i.e., the polyampholyte

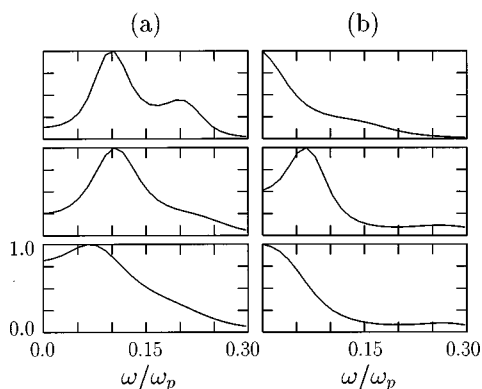


FIG. 13. Frequency spectral analysis with the maximum entropy method for the gyration radius of six 32-mer polyampholyte at (a) high temperature  $T/T_0=1$  and (b) low temperature  $T/T_0=1/8$ . Each frame corresponds to one specific chain.

density is constant. This has the effect of maintaining the Coulomb interaction at the same level. The system gyration radius of an eight-chain polyampholyte is slightly larger than that of a four-chain polyampholyte in the temperature range of  $0.1 < T/T_0 < 1$ . This is rather straightforward, since a larger number of chains means more freedom for the conformational organization. Accordingly, the filling index decreases as the number of chains increases in the above temperature range.

However, the dependence on the number of chains becomes almost invisible when the molecular weight of the chains is kept the same. In this case, the freedom for expansion due to the increase in the number of the chains may be compensated by an intensified Coulomb force that compresses the polyampholyte.

#### F. Oscillations in multichain polyampholytes

When we take a precise look at the motion of individual chains, we find slow oscillations in the gyration radius and the velocity of the monomers. We note in passing that the eigen oscillations are suppressed by the friction of a Langevin fluid. The slow oscillations should correspond to transformation of the conformation between elongated coils and a loose globule; this is inferred by comparison of the snapshots (b) and (c) of Fig. 1 (the oscillatory motions are clearly seen in a video movie). A spectral analysis of the time series data of the gyration radius  $R_{g1}$  was made with the use of the maximum entropy method.<sup>20</sup> The maximum entropy method is a very powerful tool for spectral analysis of nonstationary quantities under growth or attenuation. (The spectral peaks are obtained with high accuracy, but the height of the peaks does not correspond to the power spectral density.) Figure 13 shows that the chains undergo slow oscillations. At high temperature, we see oscillations in most of the chains that are separated from each other. The period of oscillations has a range in value:  $\tau \sim 60 - 100\omega_p^{-1}$ . At low temperature, the chains lump up as a globule, and only a small number of chains make oscillations whose period is longer than that at high temperature.

The velocity of the sampled monomers also oscillates. At high temperature, the frequency band is broad, extending

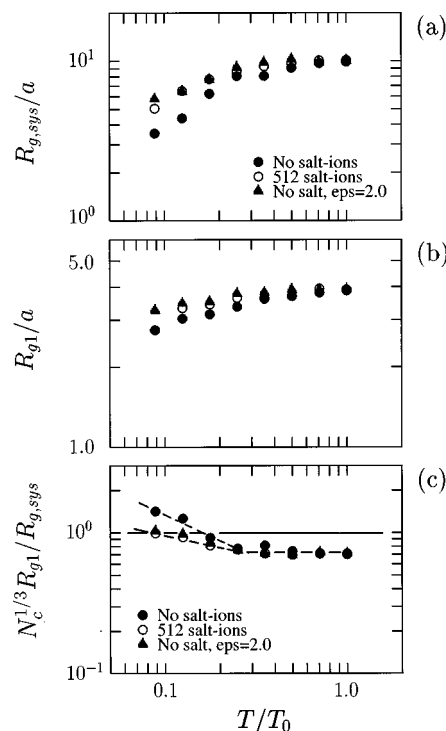


FIG. 14. Effect of salt addition for the case with 512 salt ions (256 positive and negative free ions), and for the case of enhanced electrical permittivity  $\epsilon=2\epsilon_0$  without salt ions. The polyampholyte is composed of randomly copolymerized six 32-mers, and the panels show (a) the system gyration radius  $R_{g,sys}$ , (b) the average gyration radius of the chains  $R_{g1}$ , and (c) the filling index  $N_c^{1/3} R_{g1} / R_{g,sys}$ .

over  $\tau=6-60\omega_p^{-1}$ . Only the low frequency part ( $\omega < 2\pi\nu$ ) is related to changes in the global conformation. At low temperature, the oscillations are limited to a narrow band of slow oscillations whose period is  $\tau \sim 30 - 60\omega_p^{-1}$ , implying less freedom for conformational changes.

#### IV. POLYAMPHOLYTES IN SALT-ADDED SOLUTION

Addition of salt to a solution with precipitated polyampholytes is expected to screen the internal electric field among the monomers, and to loosen the binding of the monomers within the globules, which causes dissolution of the polyampholyte.<sup>8</sup> Such effects of salt may be studied by placing free counterions in the multichain polyampholyte system. In the following run, the polyampholyte consists of six 32-mers of random copolymerization with overall charge neutrality. The initial positions of the chains are sufficiently separated such that the mass-centers of the six chains are placed at  $\pm 3.5a$  on the  $x$ ,  $y$ , and  $z$ -axis. We introduce the same number of positive and negative counterions, with their mass and charge equal to those of the chained monomers. The reflecting wall is placed at radius  $R=17.5a$  for the polyampholyte, whereas the wall is set at  $R=14a$  for the counterions for the purpose of computational efficiency. This treatment is justified since the polyampholyte is confined in the latter volume at low temperatures where the effect of added salt is most predominant.

Figure 14 shows the effect of salt (512 salt ions, with half positive ions and the other half negative ions). Each data

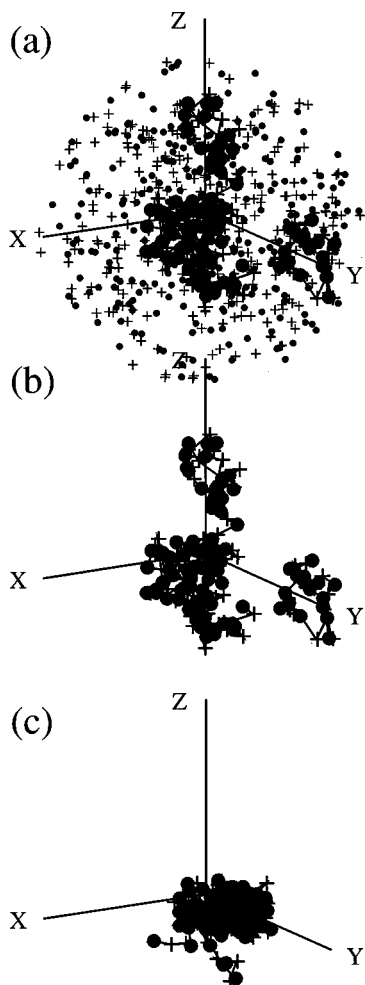


FIG. 15. Typical relaxed conformation of randomly copolymerized polyampholyte (six 32-mers) in salt-added solution for the run in Fig. 14 at temperature  $T/T_0=1/8$ : (a) polyampholyte and salt ions; (b) only the polyampholyte. The positive and negative salt ions are marked with + and ●, respectively. The relaxed conformation of the salt-free polyampholyte for the same temperature is shown in (c).

point in this figure is an average over ten independent runs with polyampholytes of different charge sequences and initial conformations. Evidently, the system gyration radius of polyampholytes increases by addition of salt, which affects preferentially the low temperature regime,  $T/T_0 \leq 0.3$  for the flexible chains ( $a_{\text{col}}=0.5a$ ). The average of the gyration radii of the individual chains becomes slightly larger in the presence of salt ions. The critical temperature at which the filling index becomes unity,  $\zeta = N_c^{1/3} R_{g1}/R_{g,\text{sys}}=1$ , is  $T_*/T_0 \sim 0.17$  in a pure solvent. After addition of salt, the filling index is reduced to less than unity in the entire temperature range shown in Fig. 14(c). This means dissolution of polyampholytes due to salt addition.

The above results indicate that the electric field binding the monomers has been screened by the salt ions. This point is directly proven by the salt-free simulation where the strength of electrical permittivity in Eq. (3) is increased to  $\epsilon=2\epsilon_0$ , with  $\epsilon_0$  the original value in the salt-free solution. The triangles in Fig. 14 depict this case with enhanced electrical permittivity, which nicely reproduces all the results for 512 salt ions.

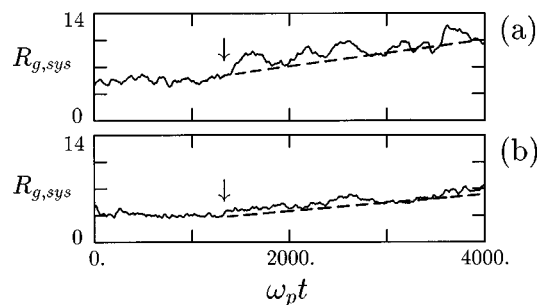


FIG. 16. Effectiveness of added salt. The system gyration radius for the runs in which 512 salt ions are placed in a region excluded by the globule of six 32-mer chains at the intermediate time  $t=1300\omega_p^{-1}$  (denoted by arrows). The temperature is (a)  $T/T_0=1/4$  and (b)  $T/T_0=1/8$ .

The density of the polyampholyte localized within the globule is  $n_{PA} \sim 0.62a^{-3}$  at  $T/T_0=1/8$ . The salt density due to 512 counterions is  $n_{\text{sal}} \sim 512/(14a)^3 \sim 0.19a^{-3}$ . The added salt, whose density is a fraction of that of the polyampholyte, is already as effective as the electrolyte solution with  $\epsilon > \epsilon_0$  in its ability to loosen the globule. This density is somewhat less than, but qualitatively in agreement with, the prediction by Higgs and Joanny.<sup>8</sup>

The typical relaxed conformation of the polyampholyte in the salt-added Langevin fluid is shown in Fig. 15(a) for  $T/T_0=1/8$ . Small pluses and dots stand for positive and negative salt ions, respectively. Figure 15(b) shows only chained monomers of the polyampholyte in Fig. 15(a). In the presence of salt, a mixture of a loose globule and separated chains is obtained, for which  $\zeta < 1$ . For comparison, conformation of the polyampholyte in the pure solvent is shown in Fig. 15(c) for the same temperature. This dense globule is in clear contrast with the loose one in the salt-added solution.

Finally, we obtained two simulation results that reveal the subtlety of the effects of salt, especially at low temperature. First, half the number (256) of salt ions, each of which carries twice more the amount of charges, have the same effect as the standard salt of basic charge. However, for very low temperatures  $T/T_0 \leq 0.1$ , half the number of salt ions with double the charges are less effective than the standard salt ions, due to less homogeneity of the salt ions. Here a discreteness effect in the function of salt appears.

Second, when the polyampholyte chains are placed in close proximity to each other before salt addition, the size of salt-added polyampholyte does increase but very slowly. Figure 16 shows the system gyration radius for the runs in which 512 salt ions are added at the intermediate time  $t=1300\omega_p^{-1}$  in a region not occupied by the already formed globule of six 32-mers. For both the temperatures shown in the figure, the globule begins to swell upon addition of salt ions. Some of the chains are eventually separated from the globule, and the system gyration radius approaches the value of the salt-added case shown in Fig. 14. But, the expansion occurs several times slower,  $\tau_{g1} \sim 2500\omega_p^{-1}$ , than that for the case when the globule is not formed at all,  $\tau_{\text{sal}} \sim 500\omega_p^{-1}$ .

These observations are uniquely explained by the ability of salt ions to penetrate among the polyampholyte chains and globules. Namely, lighter salt ions have easier and more ho-

mogeneous access to inside the globules, with more effectiveness when the globules are less tight. The use of the continuous fluid model with enhanced electrical permittivity, i.e., nonparticle model, is thus not very accurate in these cases.

## V. SUMMARY AND CONCLUSION

In this paper, the multichain effect and also that of added salt on randomly copolymerized polyampholytes have been studied. For high temperature, a container-bound one-phase state with homogeneously scattered chains is obtained due to confinement in the finite volume (Fig. 1). Polyampholyte expansion occurs in about 5% of the thermal speed on average; the typical expansion time is  $\tau \sim 300\omega_p^{-1}$  (Fig. 2), which corresponds to a few tens of picoseconds for the  $\text{CH}_2$  monomers in pure water. The size of a multichain polyampholyte becomes much greater than that of a single-chain polyampholyte at high temperature, due to the growth of a large void space among the chains (Fig. 3).

At medium and low temperature, the role of the Coulomb force, which is attractive on average, is predominant; the monomers tend to associate and form loose complexes (Figs. 3 and 4). The association and dissociation processes occur repeatedly at medium temperature, where the former process occurs a few times faster than the latter (Fig. 9). As temperature is lowered (which corresponds to density rising in experiments), a glass transition takes place. At very low temperature, a compact globule in the state of glass with a distinct round surface is formed both for the single and multichain polyampholytes. The entanglement of the chains without actual bonds between the chain elements is not enough to sustain the globule; the monomers in the globule diffuse away when the Coulomb force is switched off (Fig. 10).

The stationary globular state at low temperature is thought to arise from enhanced stability by charge pairing (Table I). An increase in temperature removes the pairing, and the globular state is lost by thermal agitation. Although the MD simulation time is restrictive to see a real long-time behavior of the polyampholyte chains, an estimate of the lifetime of a collapsed globule by Eqs. (12)–(16) tells that its life is very long, which would be destroyed only after a passage of an astronomical time. The initial conformations are either on the globule (glass) regime or the coil regime, depending on their volume [cf. Eq. (13)]. The probability for the compact globule to be destroyed and transformed to an assembly of scattered chains is estimated to be  $P_{\text{dis}} = \exp(-\Delta E/k_B T) \sim \exp(-N^{3/2})$  [Eq. (15)], which is infinitesimally small for any realistic value for the number of monomers  $N$ . The compact globule is considered to be a natural state in the low temperature regime, irrespective of the boundary condition of the domain (Fig. 8).

A good index to measure the denseness of monomers, or the degree of chain entanglement, is the filling index, defined by  $\zeta \equiv N_c^{1/3} R_{g1} / R_{g,\text{sys}}$ , with  $N_c$  the number of chains, and  $R_{g1}$  and  $R_{g,\text{sys}}$  the gyration radii of an individual chain and the whole polyampholyte, respectively. The filling index is comparable to or exceeds unity when the chains closely

overlap and become entangled. Polyampholytes become more dense when the chain stiffness or the molecular weight of the chains is increased (Figs. 5 and 11), whereas they become sparse when the number of chains is increased, though to a lesser degree (Fig. 12).

The critical temperature that separates the one-phase state with scattered chains and the segregated phase with a globule is defined by the condition that the filling index becomes unity:  $\zeta = 1$ . The critical temperature is well fitted by  $T_*/T_0 \propto M_w$ , with  $M_w$  the molecular weight of the chain. A polyampholyte consisting of chains of larger molecular weight is shown to be more difficult to dissolve in salt-free solvents.

The polyampholytes with alternating sequences of positive and negative monomers generally occupy larger volume than do the randomly copolymerized ones (Fig. 7), because the electric field is spatially averaged out. However, such effects are apparent only when the block size of alternating sequences is as small as two. Otherwise, the polyampholytes with alternating sequences behave like randomly copolymerized polyampholytes.

The size of polyampholytes is affected by the domain size at high temperature where a confining wall (container) limits their diffusion, while it is not at low temperature (Fig. 8). A glasslike compact globule is a natural state of the low temperature regime, as stated above. The results for polyampholytes under the periodic boundary conditions<sup>15</sup> are qualitatively the same as those of isolated (container bound) polyampholytes which were studied in this paper.

Spectral analysis shows slow oscillations of the chains of multichain polyampholytes at high temperature, which corresponds to transformation of the conformation between elongated coils and a loose globule (Fig. 13). At low temperature, the oscillation of individual chains is not prominent since all the chains are contained in the dense globule. However, the chained monomers are still under thermal vibrations, showing the glasslike nature of the globule [also, Fig. 6(b)].

Concerning the effect of added salt, the salt ions diffuse among the monomers of polyampholytes and screen the internal electric field, which loosens and destroys the insoluble globules at low temperature (Fig. 15). The salt, whose density reaches a fraction of that of the polyampholyte, behaves like an electrolyte solution that has enhanced electrical permittivity compared to a salt-free solution (Fig. 14). This behavior is in agreement with theory,<sup>8</sup> although the salt concentration required for dissolution of the globule is less than that predicted by the theory.

However, the effectiveness of salt is suppressed when the size of salt ions is appreciable with respect to polyampholyte chains, or when dense globules have been formed before the addition of salt (Fig. 16). The use of the continuous fluid model with enhanced electrical permittivity is shown to be inaccurate to trace such dynamical processes. In these cases, the salt ions cannot penetrate efficiently into the globules, which makes salt less effective to shield the internal electric field that binds multichain polyampholytes.

## ACKNOWLEDGMENTS

The authors, especially M.T., would like to thank Dr. J.-F. Joanny and Dr. S. J. Candau for fruitful discussions and also warm hospitality during his visit to Strasbourg. He is grateful to Dr. T. Hatori for constructive physics discussions, and to Dr. I. Ohmine, Dr. M. Doi, and Dr. K. Yoshikawa, for their interest in the present study. Finally, neat English correction by Dr. J. W. Van Dam is gratefully acknowledged.

<sup>1</sup>C. Tanford, *Physical Chemistry of Macromolecules* (Wiley, New York, 1961).

<sup>2</sup>*Protein Folding*, edited by L. M. Gierasch and J. King (American Association for Advancement of Science, Washington D.C., 1989).

<sup>3</sup>*Polyelectrolytes* edited by M. Hara (Marcel Dekker, New York, 1993).

<sup>4</sup>F. Candau and J. F. Joanny, *Encyclopedia of Polymeric Materials*, edited by J. C. Salomone (CRC, Boca Raton, 1996), Vol. 7, pg. 5476.

<sup>5</sup>M. Mezard, G. Parisi, and M. Virasolo, *Spin Glass Theory and Beyond* (World Scientific, Singapore, 1987).

<sup>6</sup>J. M. Corpart and F. Candau, *Macromolecules* **26**, 1333 (1993).

<sup>7</sup>A. Ohlemacher, F. Candau, J. P. Munch, and S. J. Candau, *J. Polym. Sci., Part B: Polym. Phys.* **34**, 2747 (1996).

<sup>8</sup>P. G. Higgs and J.-F. Joanny, *J. Chem. Phys.* **94**, 1543 (1990).

<sup>9</sup>Y. Kantor, M. Kardar, and H. Li, *Phys. Rev. E* **49**, 1383 (1994).

<sup>10</sup>A. V. Dobrynin and M. Rubinstein, *J. Phys. II* **5**, 677 (1995).

<sup>11</sup>R. Everaers, A. Johner, and J.-F. Joanny, *Europhys. Lett.* **37**, 275 (1997); *Macromolecules* **30**, 8478 (1997).

<sup>12</sup>V. S. Pande, A. Yu. Grosberg, C. Joerg, M. Kardar, and T. Tanaka, *Phys. Rev. Lett.* **77**, 3565 (1996).

<sup>13</sup>M. Tanaka, A. Yu Grosberg, V. S. Pande, and T. Tanaka, *Phys. Rev. E* **56**, 5798 (1997).

<sup>14</sup>T. Soddemann, H. Shiessel, and A. Blumen, *Phys. Rev. E* **57**, 2081 (1998).

<sup>15</sup>M. Tanaka, A. Yu Grosberg, and T. Tanaka, in *Slow Dynamics in Complex Systems*, edited by M. Tokuyama and I. Oppenheim (AIP Conference Series, New York, 1999).

<sup>16</sup>H. Petersen, *J. Chem. Phys.* **103**, 3668 (1995).

<sup>17</sup>M. Deserno and C. Holm, *J. Chem. Phys.* **109**, 7678 (1998).

<sup>18</sup>A. Y. Grosberg and A. R. Khokhlov, *Statistical Physics of Macromolecules* (AIP, New York, 1994).

<sup>19</sup>C. Kittel and H. Kroemer, *Thermal Physics* (Freeman and Co., San Francisco, 1980).

<sup>20</sup>S. M. Kaye and S. L. Marple, *Proc. IEEE* **69**, 1380 (1981).